

RESEARCH ARTICLE

View Article Online
View Journal | View IssueCite this: *Org. Chem. Front.*, 2025, **12**, 6094

Intramolecular exciplex formation between pyrene and tetraazapyrene in supramolecular assemblies†

Xinyi Liu,^a Camila Negrete-Vergara,^{id}^a Simon M. Langenegger,^{id}^a Lorraine A. Malaspina,^b Simon Grabowsky,^{id}^b Robert Häner^{id}^{*a} and Shi-Xia Liu^{id}^{*a}

Tetraazapyrene (TAP), a nitrogen-substituted analogue of pyrene, features a planar and electron-deficient π -conjugation system, and thus can act as a π -electron-acceptor. Despite its unique electronic properties, it remains underexplored due to synthetic challenges and limited derivatization methodologies. Herein, we report the first report of the selective cascade bromination of the TAP core in the presence of dibromoisocyanuric acid, affording 4,9-dibromo-TAP as a key intermediate. This precursor was subsequently employed to construct a novel pyrene-TAP-pyrene trimer (**1**), in which a central TAP core is flanked by two pyrene units *via* phosphodiester linkages. Similar to its all-pyrene-based analog in aqueous medium, this trimer undergoes temperature-triggered self-assembly *via* inter- and intramolecular non-covalent interactions, leading to the formation of supramolecular polymers featured with a donor-acceptor-donor architecture. Upon self-assembly, trimer **1** exhibits distinct optical responses, including enhanced monomeric pyrene fluorescence and unique exciplex emission. These phenomena are attributed to enhanced electronic interactions between pyrene and TAP cores facilitated by their close spatial arrangement in the resulting nanostructures. Our findings demonstrate the reversible and tunable nature of self-assembled nanostructures, highlighting their potential in the development of stimuli-responsive materials.

Received 25th June 2025,
Accepted 23rd July 2025

DOI: 10.1039/d5qo00941c

rsc.li/frontiers-organic

Introduction

π -Conjugated systems have garnered significant attention due to their tunable molecular structures and outstanding optoelectronic properties, which make them promising candidates for a variety of electronic and photonic applications.^{1–3} Among them, polycyclic aromatic hydrocarbons (PAHs) represent an essential class of π -conjugated organic compounds, consisting of multiple fused aromatic rings that contribute to extended π -electron delocalization and unique electronic characteristics.^{4,5} The structural diversity and rigidity of PAHs allow for precise control over their electronic behavior, rendering them appealing in the development of organic semiconductors, light-emitting diodes, and photovoltaic devices.^{6–8} Tetraazapyrene (TAP), a nitrogen-substituted analogue of

pyrene as a prototype of N-PAHs, is an electron-deficient n-type semiconductor.⁹ Compared to pyrene, TAP has been largely unexplored since its initial preparation due to difficulties in synthesis and further derivatization.¹⁰ Additionally, the incorporation of nitrogen atoms in the aromatic framework leads to a low-lying LUMO and also red-shifted electronic transitions indicative of a low HOMO–LUMO gap. Insertion of bulky alkyl groups at the 2 and 7 positions enhances solubility while preserving the TAP's intrinsic electronic properties.^{11,12} In contrast, substitutions at the 4, 5, 9 and 10 positions significantly influence electronic characteristics. Very recently, we have demonstrated that 4,5,9,10-tetrabromo-1,3,6,8-tetraazapyrene forms a stable radical on the superconducting surface of Pb(111), leading to the formation of a 2D spin lattice and switchable topological superconductors, which is of prime importance for the development of topological quantum bits.^{13,14} However, the selective bromination of the TAP scaffold remains synthetically challenging, thereby restricting its application in advanced optoelectronic materials.

The formation of well-organized organic nanostructures at the molecular level is essential for developing high-performance organic electronic materials.^{15–23} In our previous work, a phosphodiester-linked 2,7-dialkynyl-substituted pyrene trimer was found to self-assemble into nanosheets and nanotubes²⁴ *via* intermolecular non-covalent interactions, such as electro-

^aDepartment of Chemistry, Biochemistry and Pharmaceutical Sciences, W. Inäbnit Laboratory for Molecular Quantum Materials and WSS-Research Center for Molecular Quantum Systems, University of Bern, Freiestrasse 3, 3012 Bern, Switzerland. E-mail: shi-xia.liu@unibe.ch

^bDepartment of Chemistry, Biochemistry and Pharmaceutical Sciences, University of Bern, CH 3012 Bern, Switzerland

† Electronic supplementary information (ESI) available. CCDC 2452237. For ESI and crystallographic data in CIF or other electronic format see DOI: <https://doi.org/10.1039/d5qo00941c>



static, π - π interactions, van der Waals forces, hydrogen bonds and hydrophobic effects. Similarly, supramolecular polymers (SPs) consisting of anthracene,²⁵ and phenanthrene²⁶ units were formed in aqueous media upon self-assembly, showing a variety of nanostructures, accompanied by distinct changes in their optical spectra, including absorption shifts and emission quenching. Such spectral changes are closely tied to the self-assembly process, underscoring the critical role of molecular organization in tuning optoelectronic behavior. To the best of our knowledge, SPs containing both pyrene and TAP aromatic cores, where TAP functions as a π -electron acceptor (A) and pyrene as a π -electron donor (D), have not yet been investigated, very likely due to synthetic challenges in the preparation of mixed pyrene-TAP oligomers. We are particularly interested in this unique D-A heterostructure because of several compelling factors. Upon self-assembly, D and A moieties within the resulting SPs are expected to align in a well-defined arrangement, bringing them into close spatial proximity. This precise molecular organization could enhance electronic interactions

between D and A units, potentially leading to special photo-physical properties.

Taking these points into consideration, we designed and synthesized a pyrene-TAP-pyrene trimer (**1**) featuring a D-A-D architecture. This trimer comprises a central TAP core flanked by two pyrene units, with all chromophores connected *via* phosphodiester linkages along short molecular axes, as illustrated in Chart 1. A key step in the synthetic route involves the selective bromination to prepare 4,9-dibromo-TAP using dibromoisocyanuric acid as the brominating agent. The self-assembly and disassembly behavior of **1** trimer was examined by temperature-dependent absorption and emission spectroscopy, while the formation of the SPs was corroborated by dynamic light scattering (DLS) and atomic force microscopy (AFM). Remarkably, the emergence of an exciplex emission in the SPs underlines its potential application in advanced optoelectronics.

Results and discussion

The synthetic pathway of trimer **1** is depicted in Scheme 1. The key intermediate, 4,9-dibromo-2,7-di-*tert*-butyl-1,3,6,8-tetraazapyrene (**2a**) was successfully synthesized *via* selective bromination of 2,7-di-*tert*-butyl-1,3,6,8-tetraazapyrene (*t*-Bu-TAP) in the presence of dibromoisocyanuric acid (DBI). It was purified by column chromatography from the mixture of brominated TAPs, as the regioselective dibrominated isomers **2a** and **2b**, as well as the more substituted reaction products **2c** and **2d**, were isolated (Fig. 1a). This finding is in contrast to the previously reported bromination of 2,7-bis(trifluoroalkyl)-1,3,6,8-tetraazapyrene by using DBI in concentrated sulfuric acid.⁹ In that case, only 2-fold brominated-TAP derivatives were isolated in poor yields ($\leq 20\%$) despite a large excess (8 equiv.) of DBI and a long reaction time (48 h). We investigated the effects of DBI equivalents, the reaction temperature and time to maximize the yield of **2a** (Table S1†). The reaction of *t*-Bu-TAP with 1.5 equivalents of DBI at room temperature for 20 h afforded **2a** in 37% yield, which represents the best result obtained so far.

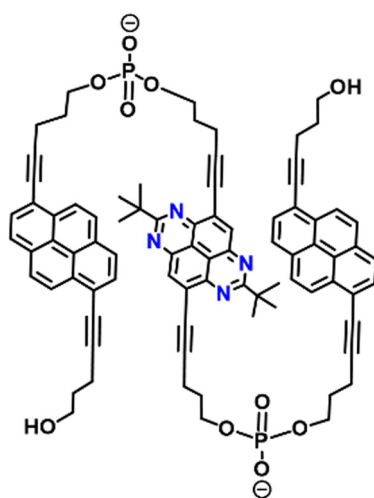
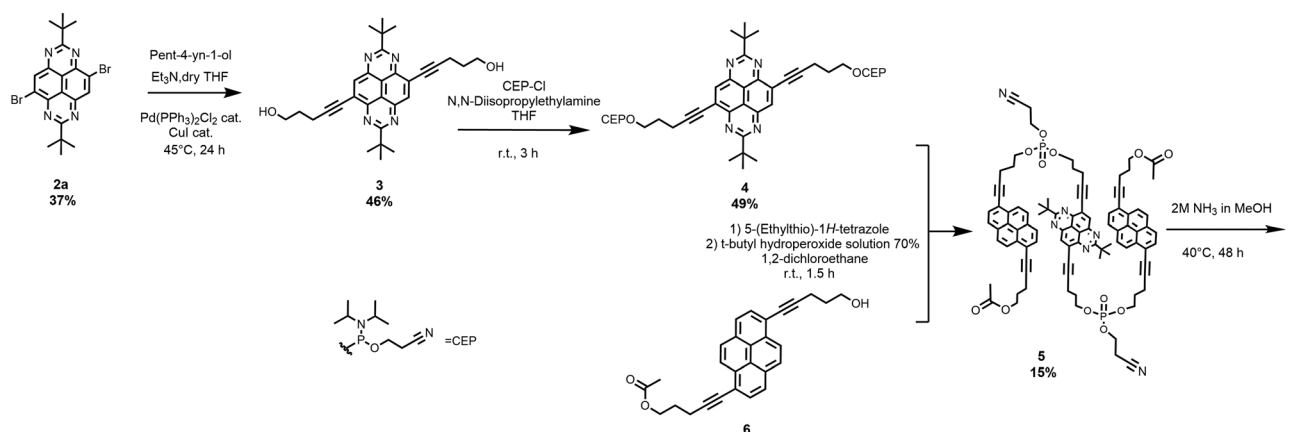


Chart 1 Chemical structure of the target trimer **1**.



Scheme 1 Synthetic route for trimer **1**.



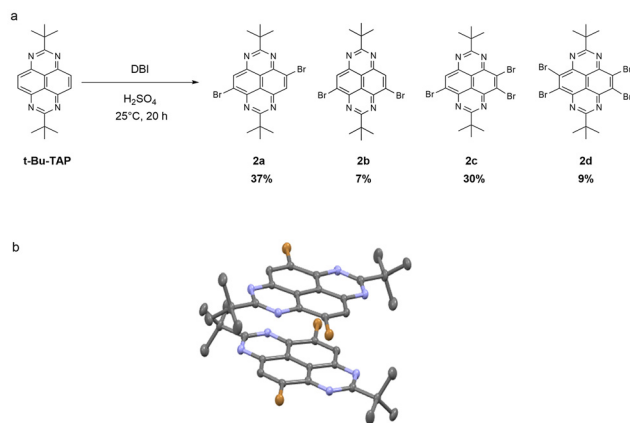


Fig. 1 (a) Synthesis of the 4,9-dibrominated precursor **2a** along with the concurrently formed isomers **2b–2d**. (b) Crystal structure of **2a** (hydrogen atoms are omitted for clarity).

The relatively low yield is mainly due to the inevitable formation of (4,10)-di-, (4,9,10)-tri- and (4,5,9,10)-tetrabrominated TAP byproducts (**2b–2d**). Remarkably, 2-fold bromination under these optimized conditions proceeds with high regioselectivity, leading to the preferential introduction of bromine atoms at the 4- and 9-positions of the TAP core, which is unambiguously confirmed by the X-ray single crystal structure shown in Fig. 1b and Fig. S2.† Single crystals of the key intermediate **2a** were obtained by solvent layering method using dichloromethane and heptane, and its structure is elucidated in Fig. S2† showing a packing diagram *via* π - π interactions (3.398 Å) and Br...Br intermolecular contacts (3.561 Å). Along the *b*-axis, the planar TAP units are orientated at an angle of 120.5° to the adjacent ones, very probably due to steric hindrance of the bulky *t*-Bu groups. They are alternately arranged at a π -stacking distance of 3.398 Å. Along the *c*-axis, the molecular arrangement is characterized by contacts between bromine atoms of two adjacent TAP molecules.

In Scheme 1, the Sonogashira coupling reaction of **2a** with pent-4-yn-1-ol, catalyzed by Pd(PPh₃)₂Cl₂ and CuI, yielded **3** in good yield. This diol was then reacted with 2-cyanoethyl-*N,N*-diisopropyl-chlorophosphoramidite (CEP-Cl) to obtain the corresponding bis-phosphoramidite (**4**) in 49% yield. Following a well-established procedure,⁹ the protected trimer **5** was readily synthesized by coupling **4** with the mono-acetylated pyrene derivative **6**²⁰ using 5-(ethylthio)-1*H*-tetrazole as the activator and then oxidized with *tert*-butyl hydroperoxide. The subsequent deprotection was accomplished by using a 2 M solution of NH₃ in MeOH at 40 °C for 48 h, resulting in the quantitative formation of the target trimer **1**. The reaction mixture was then lyophilized to afford the analytically pure trimer **1** as a yellow solid, confirmed by HPLC and MS (see ESI†).

As depicted in Fig. 2, the photophysical properties of the trimer **1** in ethanol, along with reference compounds **3** and **6**, were evaluated by absorption and emission spectroscopy. All of them absorb in the UV-visible region, which is consistent

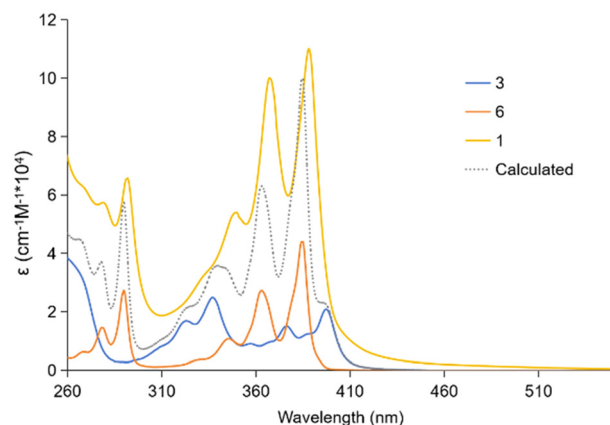


Fig. 2 UV-Vis absorption spectra of the compounds **3** (blue), **6** (orange), **1** (yellow) and the calculated spectra (the sum of **3** and **6** in a ratio of 1 : 2) (grey dotted) at a concentration of 10 μM in ethanol.

with their yellow color. Essentially, the absorption bands in the 350–420 nm region correspond to the π - π^* electronic transitions. Compared to **6** (orange curve), **3** shows a bathochromic shift of the lowest energy absorption band (blue curve), which is attributed to the low energy of the HOMO–LUMO transition because of the electron-deficient nature of the TAP core. The absorption spectrum of the trimer **1** shows a slight bathochromic shift in comparison to the calculated spectra, which is the sum of the individual spectra **6** and **3** in a ratio of 2 : 1 (Fig. 2, grey dotted curve). Upon excitation at 368 nm, **6** exhibits strong fluorescence, consistent with previously reported behavior of other pyrene derivatives^{27,28} while **3** shows almost no fluorescence (Fig. S3†). Interestingly, the molecularly dissolved trimer **1** displays an emission profile like that of **6**. All these observations suggest a weak electronic coupling between the TAP and pyrene moieties in **1** as they are linked through flexible σ -spacers.

Similar to its pyrene-based analog in aqueous medium,^{29,30} the trimer **1** undergoes temperature-dependent self-assembly under aqueous conditions, resulting in the formation of SPs. A range of experimental conditions were explored to optimize the self-assembly process. At elevated temperatures, the aggregates disassemble completely into individual trimers, which subsequently reassemble into SPs upon controlled cooling (0.1 °C min⁻¹) to room temperature. These temperature-driven self-assembly and disassembly behaviors were systematically investigated using UV-Vis absorption and emission spectroscopy, allowing to monitor spectral changes of **1** in aqueous media.

As shown in Fig. 3a, the controlled cooling of the trimer solution led to a significant decrease in the intensity of two intense absorption bands in the range of 350–400 nm by approximately 60%. This noticeable hypochromicity is indicative of the self-assembly process *via* strong π - π stacking interactions between the pyrene and TAP cores. At 75 °C, the absorption spectrum closely resembles that of individual trimers (yellow curve, Fig. 2), as explicitly demonstrated by



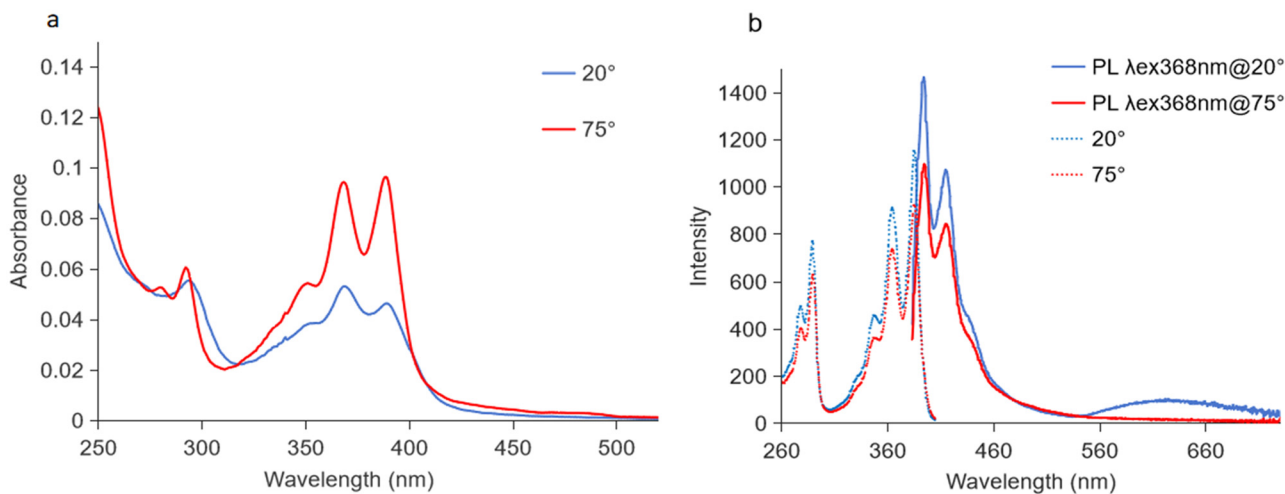


Fig. 3 (a) UV-Vis absorption spectra of **1** at 20 °C (red) and 75 °C (blue) and (b) fluorescence (solid line, $\lambda_{\text{ex}} = 368$ nm) and excitation (dotted, $\lambda_{\text{em}} = 415$ nm) spectra of **1** at 75 °C (red) and 20 °C (blue). Conditions: 1 μM **1**, 10 mM sodium phosphate buffer pH 7.2, 10 mM sodium chloride, 2.5 vol% ethanol.

their overlaid spectra (Fig. S4†), indicating nearly complete disassembly of the SPs. This conclusion is further reinforced by DLS measurements at 75 °C, which show no detectable supramolecular assemblies (Fig. S5†). Upon self-assembly, the π - π^* electronic transitions are slightly red-shifted by 2 nm, indicative of proximal electronic coupling between pyrene and TAP moieties in the resulting SPs.

To gain further insight into the reversible self-assembly process, absorbance changes were monitored at the 390 nm wavelength during the cooling process (Fig. S6†). The results suggest a nucleation-elongation mechanism,^{31,32} with self-assembly starting around 65 °C and proceeding down to 55 °C, as indicated by changes in absorbance at 390 nm.

Emission spectral changes upon annealing provide further evidence for the proposed self-assembly process. At 75 °C, the molecularly dissolved trimer shows emission peaks (395 nm and 415 nm), correlating well with the monomeric pyrene (Fig. 3b red curve). Upon cooling to 20 °C, a substantial increase in the intensity of monomeric pyrene fluorescence is observed, accompanied by a slight bathochromic shift of 3 nm that correlates with the absorption features (Fig. 3a). These observations suggest restricted molecular motion and close spatial alignment of pyrene-TAP-pyrene within and between trimers. Temperature-dependent quantum yield measurements in aqueous medium ($\Phi_{\text{F}} = 55\%$ at 20 °C; $\Phi_{\text{F}} = 31\%$ at 75 °C, Table S2†) support this interpretation, revealing a moderate decrease in pyrene-based fluorescence efficiency due to thermal quenching. However, the observed changes in emission spectra are more pronounced than expected from quantum yield alone. Remarkably, a broad and structureless emission centered around 600 nm also emerges at 20 °C. This new feature indicates thermally modulated interactions between the TAP and pyrene moieties *via* self-assembly. Such interactions are consistent with the formation of an exciplex between the pyrene and TAP units, facilitated by their close

spatial arrangement in the self-assembled structure as observed in other pyrene-based systems in aqueous media.^{33–35} Further evidence stems from control experiments using a 1 : 2 mixture of compounds **3** and **6** (Fig. S7†) show no exciplex-like emission, even at high concentrations, confirming that the emission band around 600 nm predominantly arises from an intramolecular exciplex formed between the covalently linked pyrene and TAP units. Similar exciplex-based emission systems have been studied in the context of photosynthesis and photoinduced electron transfer, particularly in D-spacer-A systems designed to achieve long-lived charge-separated states, such as those incorporating porphyrins, fullerenes, and carbon nanotubes.^{36,37}

Additionally, the size of SPs formed *via* the self-assembly of trimers was measured by DLS (Fig. S5a†), indicative of a hydrodynamic radius of approximately 80 nm. The AFM image (Fig. S8†) reveals nanoscale features consistent with supramolecular assemblies, although the morphology appears irregular. This observation, together with the DLS data, supports the presence of supramolecular assemblies.

Conclusions

In summary, this study presents the first report of the selective cascade bromination of the TAP core by using DBI as the brominating agent. The newly synthesized trimer **1** exhibits distinct optical responses, including exciplex emission, driven by self-assembly *via* inter- and intramolecular non-covalent interactions in aqueous medium. While our experimental findings strongly support the formation of an exciplex, future theoretical studies could provide further insight into the excited-state electronic structure and conformational dynamics of the trimer **1**. This work highlights the reversible and tunable nature of self-assembled nanostructures, making such systems



promising for the development of stimuli-responsive materials. Particularly, the self-assembly triggered exciplex formation holds great promise for potential applications in the field of organic optoelectronics, including high-efficiency OLEDs where exciplexes act as effective co-hosts,³⁸ and organic photovoltaics, in which they facilitate charge separation in low dielectric environments.³⁹

Conflicts of interest

The authors declare no conflicts of interest. The funders had no role in the design of the study; in the collection, analyses, or interpretation of data; in the writing of the manuscript; or in the decision to publish the results.

Data availability

Detailed experimental procedures and compound characterization data, NMR, MS and optical spectra of all new compounds (PDF) as well as DLS, AFM experiments are available within the article and its ESI.† Crystallographic data for **2a** has been deposited at the CCDC under 2452237† and can be obtained from <https://www.ccdc.cam.ac.uk>.

Acknowledgements

We gratefully acknowledge the Werner Siemens Stiftung (WSS) for supporting the WSS Research Centre for Molecular Quantum Systems (molQ). Financial support by the Swiss National Foundation, grant numbers 200020_188468 and 200021_204053 as well as by the SNSF Sinergia grant CRSII5_213533 is gratefully acknowledged.

References

- 1 A. Khasbaatar, Z. Xu, J.-H. Lee, G. Campillo-Alvarado, C. Hwang, B. N. Onusaitis and Y. Diao, Molecular Assembly of π -Conjugated Systems and Impact on (Opto)electronic Properties, *Chem. Rev.*, 2023, **123**, 8395–8487.
- 2 A. L. Kanibolotsky, I. F. Perepichka and P. J. Skabara, Star-shaped p-conjugated oligomers and their applications in organic electronics and photonics, *Chem. Soc. Rev.*, 2010, **39**, 2695–2728.
- 3 D. Tuncel, p-Conjugated nanostructured materials: preparation, properties and photonic applications, *Nanoscale Adv.*, 2019, **1**, 19–33.
- 4 K. Islam, H. Narjinari and A. Kumar, Polycyclic Aromatic Hydrocarbons Bearing Polyethynyl Bridges: Synthesis, Photophysical Properties, and their Applications, *Asian J. Org. Chem.*, 2021, **10**, 1544–1566.
- 5 Q. Li, Y. Zhang, Z. Xie, Y. Zhen, W. Hu and H. Dong, Polycyclic aromatic hydrocarbon-based organic semiconductors: ring-closing synthesis and optoelectronic properties, *J. Mater. Chem. C*, 2022, **10**, 2411–2430.
- 6 J. Wagner, P. Zimmermann Crocomo, M. A. Kochman, A. Kubas, P. Data and M. Lindner, Modular Nitrogen-Doped Concave Polycyclic Aromatic Hydrocarbons for High-Performance Organic Light-Emitting Diodes with Tunable Emission Mechanisms, *Angew. Chem., Int. Ed.*, 2022, **61**, e202202232.
- 7 S. Hashimoto, T. Ikuta, K. Shiren, S. Nakatsuka, J. Ni, M. Nakamura and T. Hatakeyama, Triplet-Energy Control of Polycyclic Aromatic Hydrocarbons by BN Replacement: Development of Ambipolar Host Materials for Phosphorescent Organic Light-Emitting Diodes, *Chem. Mater.*, 2014, **26**, 6265–6271.
- 8 C. Aumaitre and J.-F. Morin, Polycyclic Aromatic Hydrocarbons as Potential Building Blocks for Organic Solar Cells, *Chem. Rec.*, 2019, **19**, 1142–1154.
- 9 S. Geib, S. C. Martens, U. Zschieschang, F. Lombeck, H. Wadepohl, H. Klauk and L. H. Gade, 1,3,6,8-Tetraazapyrenes: Synthesis, Solid-State Structures, and Properties as Redox-Active Materials, *J. Org. Chem.*, 2012, **77**, 6107–6116.
- 10 O. Dimroth and H. Roos, Das Naphtazarin und das 5,6-Dioxy-1,4-Naphtochinon, *Justus Liebigs Ann. Chem.*, 1927, **456**, 177–192.
- 11 P. Zhou, U. Aschauer, S. Decurtins, T. Feurer, R. Häner and S.-X. Liu, Effect of tert-butyl groups on electronic communication between redox units in tetrathiafulvalene-tetraazapyrene triads, *Chem. Commun.*, 2021, **57**, 12972–12975.
- 12 P. Zhou, M. N. H. Pashaki, H.-M. Frey, A. Hauser, S. Decurtins, A. Cannizzo, T. Feurer, R. Häner, U. Aschauer and S.-X. Liu, Photoinduced asymmetric charge trapping in a symmetric tetraazapyrene-fused bis(tetrathiafulvalene) conjugate, *Chem. Sci.*, 2023, **14**, 12715–12722.
- 13 C. Li, V. Pokorný, M. Žonda, J.-C. Liu, P. Zhou, O. Chahib, T. Glatzel, R. Häner, S. Decurtins, S.-X. Liu, R. Pawlak and E. Meyer, Individual Assembly of Radical Molecules on Superconductors: Demonstrating Quantum Spin Behavior and Bistable Charge Rearrangement, *ACS Nano*, 2025, **19**, 3403–3413.
- 14 C. Li, C. Kaspar, P. Zhou, J.-C. Liu, O. Chahib, T. Glatzel, R. Häner, U. Aschauer, S. Decurtins, S.-X. Liu, M. Thoss, E. Meyer and R. Pawlak, Strong signature of electron-vibration coupling in molecules on Ag (111) triggered by tip-gated discharging, *Nat. Commun.*, 2023, **14**, 5956.
- 15 X. Tian, N. A. Risgaard, P. M. G. Löffler and S. Vogel, DNA-Programmed Lipid Nanoreactors for Synthesis of Carbohydrate Mimetics by Fusion of Aqueous Sub-attoliter Compartments, *J. Am. Chem. Soc.*, 2023, **145**, 19633–19641.
- 16 T. Mondal, M. Nerantzaki, K. Flesch, C. Loth, M. Maaloum, Y. Cong, S. S. Sheiko and J.-F. Lutz, Large Sequence-Defined Supramolecules Obtained by the DNA-Guided Assembly of Biohybrid Poly(phosphodiester)s, *Macromolecules*, 2021, **54**, 3423–3429.
- 17 S. P. W. Wijnands, E. W. Meijer and M. Merckx, DNA-Functionalized Supramolecular Polymers: Dynamic



- Multicomponent Assemblies with Emergent Properties, *Bioconjugate Chem.*, 2019, **30**, 1905–1914.
- 18 T. Aida, E. W. Meijer and S. I. Stupp, Functional Supramolecular Polymers, *Science*, 2012, **335**, 813–817.
- 19 L. Yang, X. Tan, Z. Wang and X. Zhang, Supramolecular Polymers: Historical Development, Preparation, Characterization, and Functions, *Chem. Rev.*, 2015, **115**, 7196–7239.
- 20 N. Appukutti, A. H. de Vries, P. G. Gudeangadi, B. R. Claringbold, M. D. Garrett, M. R. Reithofer and C. J. Serpel, Sequence-complementarity dependent co-assembly of phosphodiester-linked aromatic donor-acceptor trimers, *Chem. Commun.*, 2022, **58**, 12200–12203.
- 21 N. Appukutti and C. J. Serpell, High definition polyphosphoesters: between nucleic acids and plastics, *Polym. Chem.*, 2018, **9**, 2210–2226.
- 22 E. Stulz, Nanoarchitectonics with Porphyrin Functionalized DNA, *Acc. Chem. Res.*, 2017, **50**, 823–831.
- 23 J. Gorman, S. R. E. Osborne, A. Sridhar, R. Pandya, P. Budden, A. Ohmann, N. A. Panjwani, Y. Liu, R. Collepardo-Guevara, E. Stulz and R. H. Friend, Deoxyribonucleic Acid Encoded and Size-Defined π -Stacking of Perylene Diimides, *J. Am. Chem. Soc.*, 2022, **144**, 368–376.
- 24 M. Vybornyi, Y. B.-C. Hechevarria, M. Glauser, A. V. Rudnev and R. Häner, Tubes or sheets: divergent aggregation pathways of an amphiphilic 2,7-substituted pyrene trimer, *Chem. Commun.*, 2015, **51**, 16191–16193.
- 25 H. Yu, M. Sabetti and R. Häner, Formation of Supramolecular Nanotubes by Self-assembly of a Phosphate-linked Dimeric Anthracene in Water, *Chem. – Asian J.*, 2018, **13**, 968–971.
- 26 S. M. Langenegger and R. Häner, DNA containing phenanthroline- and phenanthrene-derived, non-nucleosidic base surrogates, *Tetrahedron Lett.*, 2004, **45**, 9273–9276.
- 27 X.-Y. Wang, J. Zhang, J. Yin and S. H. Liu, Multiple Photoluminescent Processes from Pyrene Derivatives with Aggregation- and Mechano-Induced Excimer Emission, *Chem. – Asian J.*, 2019, **14**, 2903–2910.
- 28 Y. Wu, J. Wang, F. Zeng, S. Huang, J. Huang, H. Xie, C. Yu and S. Wu, Pyrene Derivative Emitting Red or near-Infrared Light with Monomer/Excimer Conversion and Its Application to Ratiometric Detection of Hypochlorite, *ACS Appl. Mater. Interfaces*, 2016, **8**, 1511–1519.
- 29 J. Thiede, S. Rothenbühler, I. Iacovache, S. M. Langenegger, B. Zuber and R. Häner, Supramolecular assembly of pyrene–DNA conjugates: influence of pyrene substitution pattern and implications for artificial LHCs, *Org. Biomol. Chem.*, 2023, **21**, 7908–7912.
- 30 E. Ehret, I. Iacovache, S. M. Langenegger, B. Zuber and R. Häner, Nanostructural diversity: self-assembly of isomeric pyrene–cholane amphiphiles into sheets, tubes, and worm-like morphologies, *RSC Adv.*, 2024, **14**, 31498–31501.
- 31 A. V. Rudnev, V. L. Malinovskii, A. L. Nussbaumer, A. Mishchenko, R. Häner and T. Wandlowski, Cooperative and Noncooperative Assembly of Oligopyrenotides Resolved by Atomic Force Microscopy, *Macromolecules*, 2012, **45**, 5986–5992.
- 32 A. Al Ouahabi, L. Charles and J.-F. Lutz, Synthesis of Non-Natural Sequence-Encoded Polymers Using Phosphoramidite Chemistry, *J. Am. Chem. Soc.*, 2015, **137**, 5629–5635.
- 33 I. Trkulja and R. Häner, Triple-Helix Mediated Excimer and Exciplex Formation, *Bioconjugate Chem.*, 2007, **18**, 289–292.
- 34 F. Garo and R. Häner, Influence of a GC Base Pair on Excitation Energy Transfer in DNAAssembled Phenanthrene π -Stacks, *Angew. Chem., Int. Ed.*, 2012, **51**, 916–919.
- 35 J. Baek, T. Umeyama, K. Stranius, H. Yamada, N. V. Tkachenko and H. Imahori, Long-Range Observation of Exciplex Formation and Decay Mediated by One-Dimensional Bridges, *J. Phys. Chem. C*, 2017, **121**, 13952–13961.
- 36 E. V. Bichenkova, A. R. Sardarian, A. N. Wilton, P. Bonnet, R. A. Bryce and K. T. Douglas, Exciplex fluorescence emission from simple organic intramolecular constructs in non-polar and highly polar media as model systems for DNA-assembled exciplex detectors, *Org. Biomol. Chem.*, 2006, **4**, 367–378.
- 37 T.-L. Wu, S.-Y. Liao, P.-Y. Huang, Z.-S. Hong, M.-P. Huang, C.-C. Lin, M.-J. Cheng and C.-H. Cheng, Exciplex Organic Light-Emitting Diodes with Nearly 20% External Quantum Efficiency: Effect of Intermolecular Steric Hindrance between the Donor and Acceptor Pair, *ACS Appl. Mater. Interfaces*, 2019, **11**, 19294–19300.
- 38 Q. Wang, Q.-S. Tian, Y.-L. Zhang, X. Tang and L.-S. Liao, High-efficiency organic light-emitting diodes with exciplex hosts, *J. Mater. Chem. C*, 2019, **7**, 11329–11360.
- 39 E. Sebastian, J. Sunny and M. Hariharan, Excimer evolution hampers symmetry-broken charge-separated states, *Chem. Sci.*, 2022, **13**, 10824–10835.

